

Article

Analysis of the Distribution Pattern of Asparagus in China Under Climate Change Based on a Parameter-Optimized MaxEnt Model

Qiliang Yang ^{1,2,3,4}, Chunwei Ji ^{1,2,3,4}, Na Li ^{1,2,3,4,*}, Haixia Lin ⁵, Mengchun Li ^{1,2,3,4}, Haojie Li ^{1,2,3,4}, Saiji Heng ^{1,2,3,4} and Jiaping Liang ^{1,2,3,4,*}

¹ Faculty of Modern Agricultural Engineering, Kunming University of Science and Technology, Kunming 650500, China

² International Joint Laboratory of Intelligent Agricultural Engineering Technology and Equipment in Yunnan Province, Kunming 650500, China

³ Yunnan Provincial Field Scientific Observation and Research Station on Water-Soil-Crop System in Seasonal Arid Region, Kunming University of Science and Technology, Kunming 650500, China

⁴ Key Laboratory of Efficient Utilisation of Agricultural Water Resources and Intelligent Control in Yunnan Province, Kunming 650500, China

⁵ College of Water Conservancy and Architectural Engineering, Shihezi University, Shihezi 832003, China

* Correspondence: lina_nafu1221@163.com (N.L.); liangjpxaut@163.com (J.L.)

Abstract: Asparagus (*Asparagus officinalis* L.) has high health and nutritional values, but the lack of scientific and rational cultivation planning has resulted in a decline in asparagus quality and yield. Important soil, climatic, anthropogenic, and topographic environmental factors influencing the distribution of asparagus cultivation were chosen for this study. The Kuenm package in the R language (v4.2.1) was employed to optimize the maximum entropy model (MaxEnt). Pearson's correlation analysis, optimized MaxEnt, and geographic information spatial technology were then utilized to identify the main environmental factors that influence suitable habitats for asparagus in China. Potential distribution patterns, migration, and changes in trends concerning the suitability of asparagus in China under various historical and future climate scenarios were modeled and projected. Human activities and climate factors were found to be the primary environmental factors that influence the suitability distribution of asparagus cultivation in China, followed by soil and topographic factors. Historical suitable habitats covered 345.6×10^5 km², accounting for 36% of China. These habitats are projected to expand considerably under future climatic conditions. This research offers a basis for the rational planning and sustainable development of asparagus cultivation.

Keywords: asparagus; climate change; human activities; model parameter optimization; habitat suitability

Academic Editors: Gniewko Niedbała

Received: 19 November 2024

Revised: 23 December 2024

Accepted: 17 January 2025

Published: 31 January 2025

Citation: Yang, Q.; Ji, C.; Li, N.; Lin, H.; Li, M.; Li, H.; Heng, S.; Liang, J. Analysis of the Distribution Pattern of Asparagus in China Under Climate Change Based on a Parameter-Optimized MaxEnt Model.

Agriculture **2025**, *15*, 320. <https://doi.org/10.3390/agriculture15030320>

Copyright: © 2025 by the authors. Licensee MDPI, Basel, Switzerland. This article is an open access article distributed under the terms and conditions of the Creative Commons Attribution (CC BY) license (<https://creativecommons.org/licenses/by/4.0/>).

1. Introduction

Asparagus (*Asparagus officinalis* L.) is a highly economical and nutritional vegetable, which contains more protein and vitamins than general vegetables. It has anti-cancer and immune-enhancing health functions and enjoys the reputation of being the “King of Vegetables” [1–4]. China is a major producer of asparagus, with the largest area and output in the world, and it acts as a critical player in the global asparagus trade [5]. After nearly 30 years of development, China's asparagus industry has developed into an emerging

industry with competitive advantages. However, asparagus planting planning and introduction cultivation are carried out blindly and at random due to the lack of guidance from scientific theory, resulting in a decline in asparagus yield and quality [6].

Species geographical distribution is affected by the combination of topography, climate, soil, and human activities [7]. The global climate has been warming since the 20th century. According to the Sixth Assessment Report of the Intergovernmental Panel on Climate Change (IPCC), the global surface temperature rose by 0.99 °C between 2001 and 2020 in contrast to 1850–1900. In 2021–2024, the temperature rise is expected to approach or surpass 1.5 °C [8]. Agriculture is one of the areas most impacted by changes in climate, largely due to the fact that heat is the energy source of crops and water is the basic component of crops, which both affect their physiological activities [9]. Higher temperatures result in a greater water vapor content in the atmosphere, a change in precipitation patterns, an increase in the frequency of extreme weather events, and changes in crop planting layouts [10].

Climate change is significantly altering species' geographical distributions, with many species shifting their ranges northward or migrating to higher elevations due to a more pronounced trend of temperature increases at higher elevations compared to lower elevations [11,12]. Comparing the past and present vegetation distribution in the Montseny Mountains in Spain, it was found that cold temperate ecosystems had been gradually replaced by Mediterranean ecosystems due to climatic warming, and beech forests had migrated to higher altitudes, with an increase of about 70 m [13]. Climate change has caused a considerable northward shift in China's prospective single-cropping and double-cropping rice planting boundaries [14]. Soil texture, chemical and physical characteristics, nutrients, and moisture influence the growth of crop roots, as well as the storage, transformation, and uptake of nutrients, thus affecting the process of crop growth, development, yield, and quality and restricting the scope of crop cultivation and distribution [15]. For example, clay soil has a strong water retention capacity and poor air permeability, resulting in long-term water retention in the soil, which can provide a good water supply for plants, so it is suitable for moisture-tolerant plants, while sandy soils have good water permeability and are suitable for growing drought-loving plants. Topography affects the distribution of hydrothermal resources, and major ecological factors like water vapor, heat, light, and soil change regularly with variations in elevation, slope, and slope direction, thus having a significant impact on crop distribution patterns [16]. Human actions, including choosing drought-tolerant crops based on the distance of water sources and transforming converted land into construction land, also significantly affect crop planting layout [17].

Species distribution models (SDMs) quantify the link between environmental parameters and species distribution, reflecting the limiting constraints of species dispersion and habitat adaptation [18]. They have been extensively utilized to model and forecast potential appropriate areas for crops, distribution patterns, and responses to the change in climate [19]. Currently, commonly used SDMs include the genetic algorithm for rule-set prediction (GARP), the bioclimate envelope model (BIOCLIM), ecological niche factor analysis (ENFA), and the maximum entropy model (MaxEnt) [20]. Among them, the MaxEnt model is the most popular and well-known model of species distribution, and it has high accuracy because of its low sample size requirements, short running time, high simulation accuracy, and outstanding predictive ability. The MaxEnt model functions on the basis of the maximum entropy principle, which uses environmental factors as constraints to identify the likelihood of maximum entropy and a functional connection established by the actual species distribution points to forecast the probable distribution of a species. The ecological niche models of Domain, BIOCLIM, MaxEnt, and GARP were employed to simulate the habitat distribution of various species at various sizes. The findings suggested

that the MaxEnt model was the most predictive for species with limited distribution data and short geographic ranges [21]. Elith et al. [22] identified that the MaxEnt model had the best performance in their simulation of the geographical distribution of 226 species over six areas of the world utilizing 16 SDMs.

MaxEnt has been extended from the simulation of potential habitats for endangered or economically valuable species and invasive species to the study of agricultural crops, such as the study of growth zonation and the assessment of response to dominant environmental factors of rice, maize, wheat, and potato [23–25], which offers an essential scientific foundation for agricultural cultivation, conservation, as well as sustainable development. The MaxEnt model was exploited to simulate and examine the impact of future climate change on maize suitability zones in Kenya. It was discovered that future climate change will result in a 1.9–3.9% rise in unsuitable maize regions and a 14.6–17.5% drop in moderately appropriate areas. The leading environmental factors influencing the spread of maize plantings were the mean wettest-season temperature, yearly mean temperature, and annual precipitation [26]. Predictive analysis of potential planting areas for regenerative rice and double-cropped rice in China via the MaxEnt model found that the area suitable for double-cropped rice cultivation was 130,500 ha, while the area suitable for growing regenerative rice was 56,400 ha. The main environmental factors that affect the suitable area for regenerating rice are average temperature in the warmest season, ≥ 10 °C cumulative temperature, annual precipitation, altitude, and annual sunshine duration [27]. The MaxEnt model has been exploited in studies of species distribution prediction, but the unoptimized model prediction results may result in serious fitting biases. Model complexity, different environmental variables, and parameters affect the model performance to different degrees. Studies have shown that optimizing the model by parameter tuning can dramatically enhance the simulation accuracy of the MaxEnt model and obtain more accurate species distributions [13,28].

At present, research on crop-suitable areas based on the MaxEnt model mainly focuses on grain crops such as rice, corn, and wheat. The influencing factors are also mostly focused on the impact of climatic factors like light, temperature, water, and heat. There is no research that fully considers the influences of natural ecosystems and human activities on the distribution of asparagus cultivation [29,30]. Therefore, this study took asparagus as the research object and considered the combined effects of topography, soils, climate, and human activities; the main environmental factors influencing the appropriate distribution of asparagus were determined using the MaxEnt model. Additionally, the features of the appropriate distribution of asparagus in China under current and various future climate scenarios were projected and analyzed. The research was conducted (1) to determine key environmental factors that influence the distribution of suitable habitats for asparagus in China; (2) to test and compare the effectiveness of the optimized MaxEnt model in predicting the species' suitable habitats; (3) to predict and analyze the underlying spatial variability and geographical distribution of asparagus under various historical and future climate scenarios; and (4) to examine the variation and migration trajectories of suitable distribution centers of asparagus in China at various periods.

2. Materials and Methods

2.1. Data Sources

Distributional data of asparagus were collected from the Global Biodiversity Information Facility (<https://www.gbif.org> (accessed on 9 May 2024)), the Chinese Virtual Herbarium (<https://www.cvh.ac.cn> (accessed on 9 May 2024)), and the National Specimen Platform (<http://www.nsii.org.cn> (accessed on 9 May 2024)). When sample records lacked detailed geographic coordinates, they were identified in Google Maps, yielding a total of 252 asparagus distribution spots [31]. The distribution point data were filtered through

the ENMTools package in R language (v4.2.1) to make sure that only one distribution point datum within a raster of 2.5' (~25 km²) precision was maintained, avoiding the overfitting of the model operation and influencing the prediction outcomes [32]. After removing the errors and repeated points, 192 asparagus distribution points were finally determined (Figure 1).

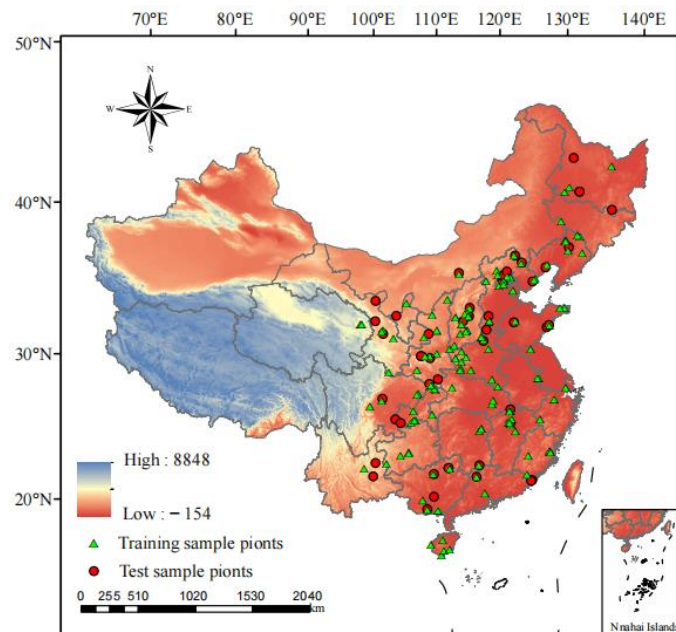


Figure 1. Asparagus distribution points in China.

Through reviewing the relevant literature, 25 environmental factors affecting asparagus planting distribution were initially screened and identified (Table 1) [33]. Terrain factors (elevation and slope) and environmental climate factors were provided by the World Climate Database (WorldClim, <http://www.worldclim.org/> (accessed on 24 May 2024)). Data on soil chemical and physical characteristics were derived from the World Soil Database (<http://www.fao.org/> (accessed on 25 May 2024)). Scenarios for future climate change consist of four shared socioeconomic pathways (SSPs), namely, SSP585, SSP370, SSP245, and SSP126, which employ the BCC-CSM2-MR climate model. Soil physicochemical property data include soil pH, organic matter, and calcium carbonate content. The anthropogenic factor is the gross domestic product (GDP) via the Chinese Academy of Science Resource and Environment Data Center (<https://www.resdc.cn/> (accessed on 25 May 2024)). Due to the limitations of the available data, the impact of factors such as GDP, soil, and terrain was only comprehensively considered during historical periods. In addition, this research mainly focused on the impact of future climate change on the suitability of asparagus planting. Therefore, it was assumed that factors such as GDP, soil, and topography would not change in the simulation study of future periods. ArcGIS 10.4 was applied to import all environmental variables for cropping and resampling, with a uniform resolution of 2.5' and the data output in ASCII format.

Table 1. Climate, soil, topography, and human activity factors affecting the distribution of asparagus planting (preliminary selection).

Type	Abbreviation	Factors	Data Sources	Year	Explanation	Unit
Climatic variables	Bio1	Annual mean temperature	WordClim: Global Climate Data Version 2.0, Web: http://www.worldclim.org/ (accessed on 24 May 2024)	1970–2000	The 19 climate factors in the WordClim climate dataset are derived from monthly precipitation values and temperature to produce more biologically significant variables, which are typically employed to model species distributions, along with the associated ecological modeling techniques. These 19 climate factors are representative of annual trends (like annual precipitation and mean annual temperature), limiting or extreme environmental factors (such as temperature in the hottest and coldest months, along with precipitation in rainy and wet months), and seasonality (like annual ranges of precipitation and temperature). A season is three months (1/4 of the year).	°C
	Bio2	Mean diurnal range				°C
	Bio3	Isothermality (Bio2/Bio7) (×100)				%
	Bio4	Temperature seasonality (standard deviation × 100)				°C
	Bio5	Max temperature of warmest month				°C
	Bio6	Min temperature of coldest month				°C
	Bio7	Temperature annual range (Bio5–Bio6)				°C
	Bio8	Mean temperature of wettest quarter				°C
	Bio9	Mean temperature of driest quarter				°C
	Bio10	Mean temperature of warmest quarter				°C
	Bio11	Mean temperature of coldest quarter				°C
	Bio12	Annual precipitation				mm
	Bio13	Precipitation of wettest month				mm
	Bio14	Precipitation of driest month				mm
	Bio15	Precipitation seasonality (coefficient of variation)				mm
	Bio16	Precipitation of wettest quarter				mm
	Bio17	Precipitation of driest quarter				mm
	Bio18	Precipitation of warmest quarter				mm
	Bio19	Precipitation of coldest quarter				mm
Terrain variables	Elevation	Altitude	WordClim: Global Climate Data Version 2.0, Web: http://www.worldclim.org/ (accessed on 24 May 2024)	1970–2000		m
	Slope	Slope				°
Human activities	GDP	Gross domestic product	Cloud Platform of the Chinese Academy of Sciences, Web: https://www.resdc.cn/ (accessed on 25 May 2024)	2010	GDP reflects the economic performance of a country or region, and economic performance is related to a variety of socioeconomic factors, which work together in the distribution of crop planting.	Ten thousand Yuan
Soil variables	pH	pH value (H ₂ O)	HWSD: Harmonized World Soil Database v2.0, Web: https://www.fao.org/soils-portal/en/ (accessed on 25 May 2024)	2010	These soil variables are directly related to the growth environment and nutrient absorption and utilization of vegetables.	–log(H ⁺)
	OC	Organic content				%
	CaCO ₃	Calcium carbonated content				%

2.2. Correlation Testing and Screening of Environmental Variables

Because there may be collinearity between the environmental variables that affect the model operation results, to prevent the MaxEnt model from overfitting, the chosen environmental variables first needed to be screened [22]. The MaxEnt model was loaded with the chosen 25 environmental variables for initial computations to obtain the rate of each variable's contribution, and Pearson correlation tests were conducted using ArcGIS (v10.4.1) and SPSS (v27.0.1) software [34]. The output of the MaxEnt simulation retains

the environmental variables with a contribution rate of over 0.1%. Multicollinearity is present when the Pearson correlation coefficient, $|r|$, between both environmental variables is over 0.8. The environmental variable that contributes more is retained, while the one that contributes less is eliminated. If both environmental variables have the same contribution rate, the variable exhibiting smaller multicollinearity with the other environmental variables is selected.

2.3. MaxEnt Model

2.3.1. Model Optimization

The MaxEnt model is prone to overfitting and sampling bias. The model transfer ability is only effective under low-threshold conditions, and default parameters can influence the prediction accuracy of the model. The complexity of the MaxEnt model is strongly correlated with its feature class (FC) and regularization factor (RM) parameters [35]. In this research, the R package Kuenm was utilized to optimize the parameters of the MaxEnt model [36]. During the optimization process, 0.1 was set as the starting value for RM, and each time, it was incremented by 0.1 up to 4.0, with a total of 40 control frequency doublings [37,38]. The optimization was carried out through combinations of five feature types: H—hinge; Q—quadratic; L—linear; T—threshold; and P—product [39]. Omission rates, along with Akaike information criterion (AICc), were employed to assess the complexity and fit of various parameter combinations of the MaxEnt model [40]. The optimal parameter value was the combination of FC and RM when the omission rates were less than 5%, the natural logarithm of AICc was the smallest, and the delta AICc values were 0 [41].

Since the area under the curve (AUC) is independent of the threshold for assessing the model's performance, the capacity of various parameter combinations to differentiate between background and test points was assayed utilizing the AUC under the receiver operating characteristic (ROC) [42].

2.3.2. Model Modeling and Accuracy Verification

The distribution data of asparagus and the selected environmental factors (GDP, Bio3, Bio5, Bio8, Bio11, Bio13, Bio14, Bio15, Bio19, CaCO₃, Eleve, pH, OC, slope) were input into MaxEnt software (v3.4.3) for model construction. The model was set to run for 10 iterations, with 75% of the data randomly chosen as the training set and the remaining 25% as the validation set. The AUC was employed to determine the prediction accuracy of the MaxEnt model, which raises as the AUC value approaches 1. $AUC \geq 0.9$, $0.8 \leq AUC < 0.9$, $0.7 \leq AUC < 0.8$, $0.6 \leq AUC < 0.7$, and $0.5 \leq AUC < 0.6$ indicate an optimal, an improved, an average, a poorer, and a failed model prediction, respectively [43].

2.3.3. Delineation and Analysis of Suitable Areas for the Cultivation of Asparagus

The "Reclassification" tool in ArcGIS was employed to categorize MaxEnt model predictions into planting suitability classes. The prediction findings of the MaxEnt model were displayed as the continuous existence probability (p), which ranges from 0 to 1 in the anticipated region. The closer the p -value is to 1, the more likely it is that the presence of the species suggests a higher degree of habitability. Taking into account the classification criteria for assessing the "likelihood" of species survival suitability developed by the IPCC, combined with the climatic conditions and planting conditions of the study area, the suitability of asparagus cultivation was divided according to the following criteria: $p < 0.08$, $0.08 \leq p < 0.27$, $0.27 \leq p < 0.86$, and $p \geq 0.86$ for unsuitable, suitable, low-suitability, moderately suitable, high-suitability planting areas, respectively. The SDMTools tool in ArcGIS software (v10.4.1) was utilized to calculate the trend of asparagus optimum areas under the impacts of historical and future changes in climate and to analyze the centroid

coordinate change and migration distance of the most suitable area [44]. The flowchart for this study is displayed in Figure 2.

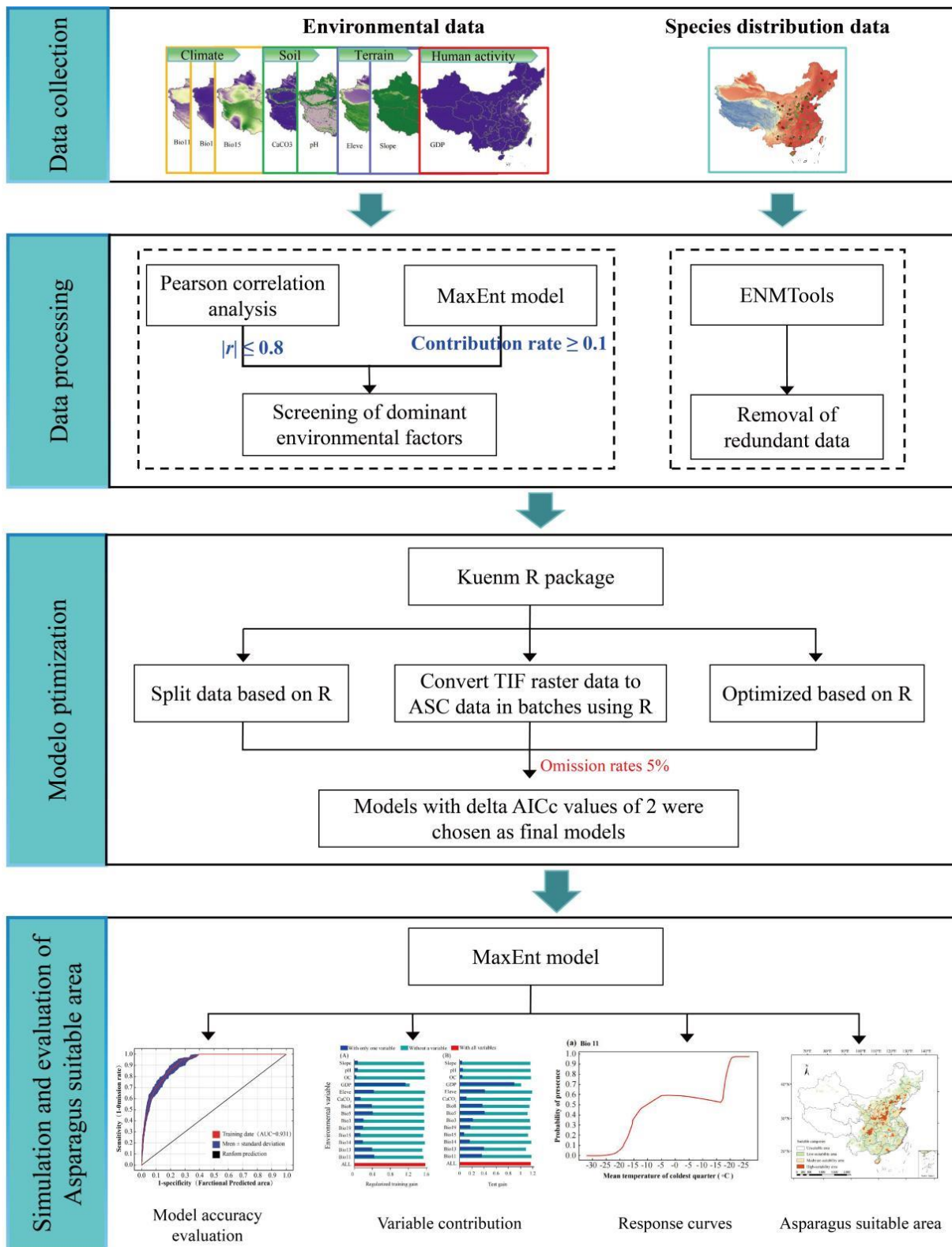


Figure 2. Methodological framework in this work.

3. Results

3.1. Optimization and Prediction Accuracy Assessment of MaxEnt Models

This study used the Kuenm package to create a total of 1160 distribution models, of which 8 met the 5% omission rate standard (Figure 3). For the optimal model, ROC = 0, omission rates = 0.04; AICc = 4968.31; and optimized model parameters RM = 0.4; and FC = FQH (Figure 3). The environmental data, along with the screened asparagus distribution data, were imported into the MaxEnt model, and the optimized parameters were repeated for 10 runs for cross-validation. According to the findings, the average AUC value of the MaxEnt model was 0.931, and its standard deviation was 0.013, indicating excellent simulation accuracy (Figure 4).

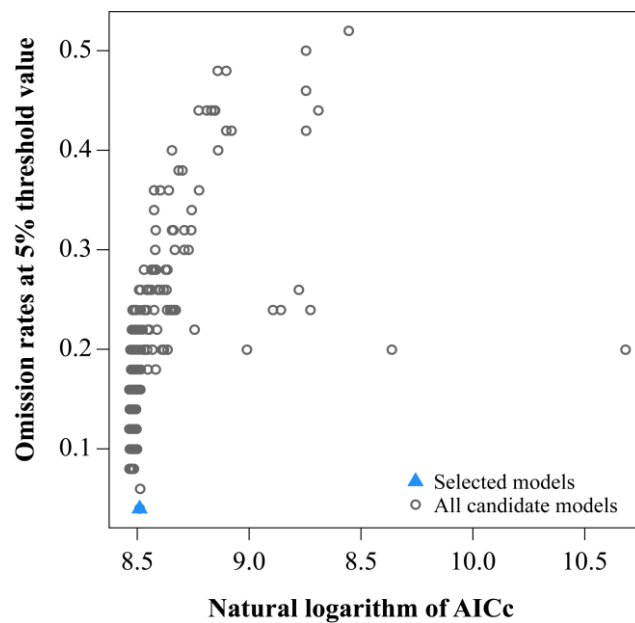


Figure 3. AICc values and omission rates for all candidate models, non-significant candidate models, and selected “best” candidate models for asparagus.

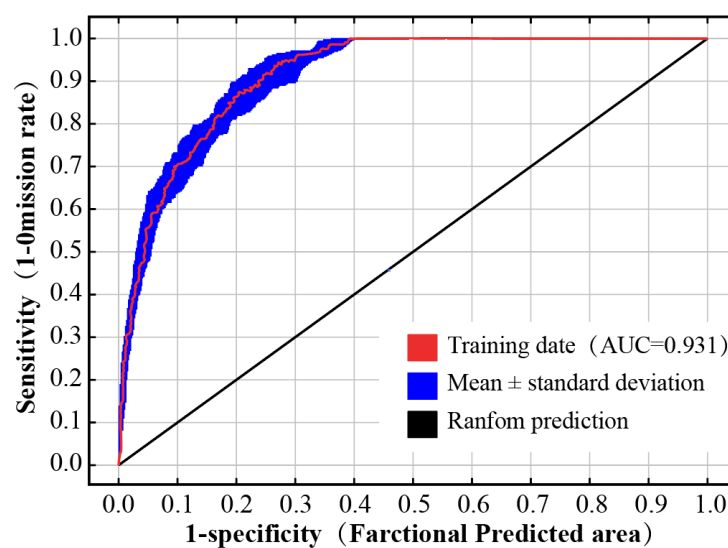


Figure 4. ROC curve for the assessment of asparagus distribution under optimal parameter conditions according to the MaxEnt model.

3.2. Screening of Main Environmental Variables

To identify the contribution rate of each factor to the asparagus cultivation distribution in China, the first 25 environmental factors were chosen and imported into the optimized MaxEnt model, and a Pearson correlation analysis was then conducted. The environmental variables with a contribution rate > 0.1% and a correlation rate < ±0.8 were screened out. In total, 14 key environmental variables that influence asparagus cultivation distribution were chosen: mean temperature in the coldest quarter (Bio11), wettest quarter (Bio8), precipitation in the wettest month (Bio13), driest month (Bio14), ratio of diurnal to annual temperature difference (Bio3), mean precipitation in the coldest quarter (Bio19), maximum temperature in the hottest month (Bio5), elevation (Eleve), soil calcium carbonated content (CaCO₃), soil pH (pH), and soil organic content (OC) (Figure 5). Compared with other environmental variables, GDP (with a contribution rate of 76.1%), Bio15 (4.5%), slope (4.3%), Bio11 (4.0%), Bio13 (2.7%), and Bio14 (2.6%) contributed the most to asparagus cultivation distribution, with a cumulative contribution rate of 94.2% (Table 2).

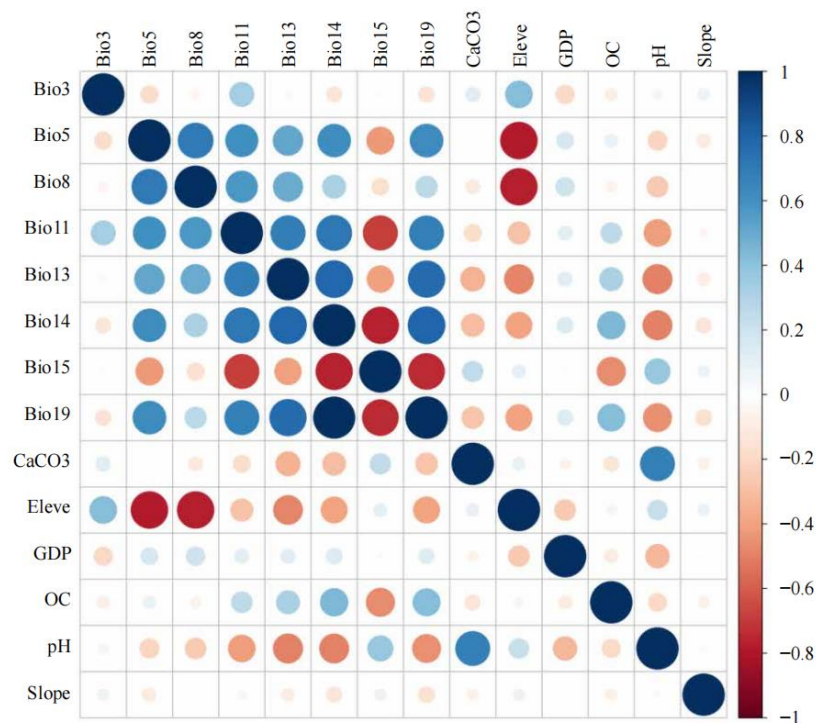


Figure 5. Correlation of initially selected environmental variables (see Table 1 for the names of the environmental factors).

Table 2. Effects of initial environmental variables on asparagus cultivation distribution in China (see Table 1 for the names of the environmental factors).

Variable	Percent Contribution (%)	Permutation Importance (%)	Variable	Percent Contribution (%)	Permutation Importance (%)
Bio1	0.2	0.1	Bio14	2.6	3.4
Bio2	0.9	0.8	Bio15	4.5	4.8
Bio3	1.8	0.9	Bio16	0.1	0.2
Bio4	1.1	3.3	Bio17	0.4	0.8
Bio5	1.6	6.5	Bio18	0.1	0.1
Bio6	1.1	0	Bio19	1.3	7.2
Bio7	2.2	0.5	GDP	71.6	41.2
Bio8	2.5	4.5	Slope	4.3	1.0
Bio9	0	0	Eleve	1.1	2.1

Bio10	0.9	2.8	CaCO ₃	1.0	2.6
Bio11	4.0	5.7	pH	0.6	1.3
Bio12	0.5	9.1	OC	0.4	1.2
Bio13	2.7	17.7			

3.3. Effect of Key Environmental Factors on the Asparagus Cultivation Distribution

According to the importance test of the Jackknife method, the significance of environment variables when there is only one environment variable is as follows: GDP > Bio11 > Elevation > Bio13 > Bio5 > Bio8 > Bio14 > Bio19 > Bio3 > Bio15 > CaCO₃ > slope > pH > OC (Figure 6). The outcomes suggested that Bio11 and GDP were the major environmental factors affecting asparagus’s geographical distribution.

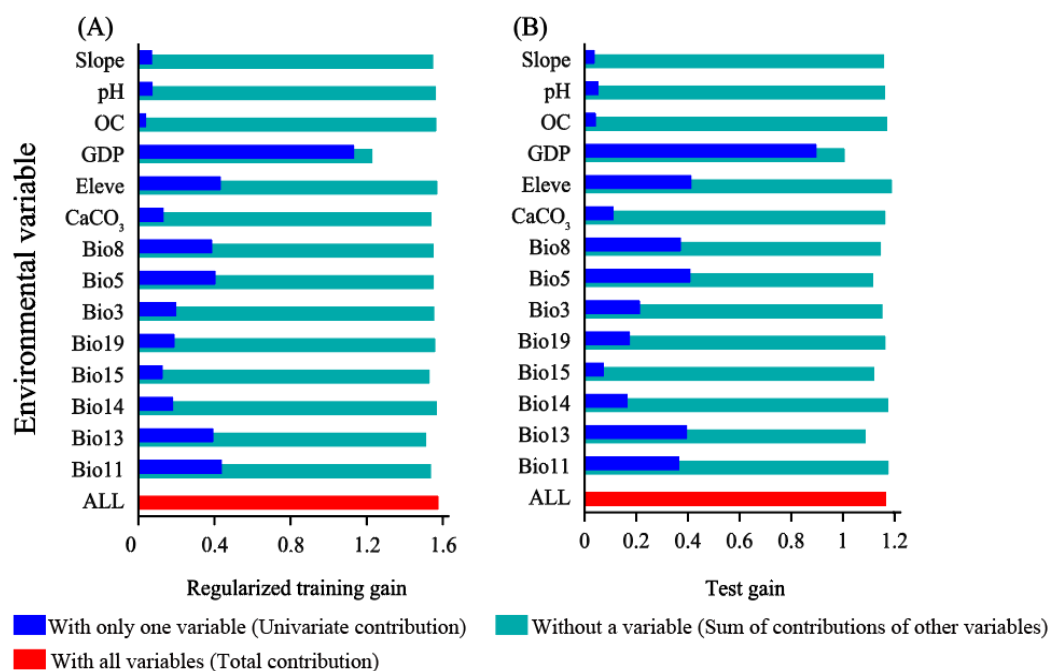


Figure 6. Jackknife test employed to establish the impact of key variables on the distribution of asparagus: (A) regularized training gain for asparagus; (B) test gain for asparagus. The impacts of the variables in the sample set were utilized for validation of the model.

Figure 7 displays the response curves of six key environmental factors (GDP, slope, Bio11, Bio13, Bio14, and Bio15) that significantly influence the suitability of asparagus cultivation in China. As the values for Bio13 and Bio14 increased, the probability of asparagus suitability experienced a sharp rise followed by a gradual decline. Specifically, the suitability probability for Bio13 peaked at approximately 0.65, with around 200 mm of precipitation, while the highest suitability for Bio14 occurred at about 20 mm of precipitation. This indicated that asparagus growth was most suitable within a certain range of precipitation. Both excessive and insufficient precipitation could reduce its growth potential. The projected non-linear relationship emphasized the water requirements of asparagus and highlighted the complex influence of precipitation on its distribution. The probability of asparagus suitability initially increased and then decreased with rising GDP, but the rate of increase and decrease was relatively slow. The highest probability of asparagus suitability was 0.85 when the GDP was 167,00.9 million yuan km⁻². The greater the slope, the lower the probability of asparagus suitability, which was below 0.5 when the slope was greater than 40°.

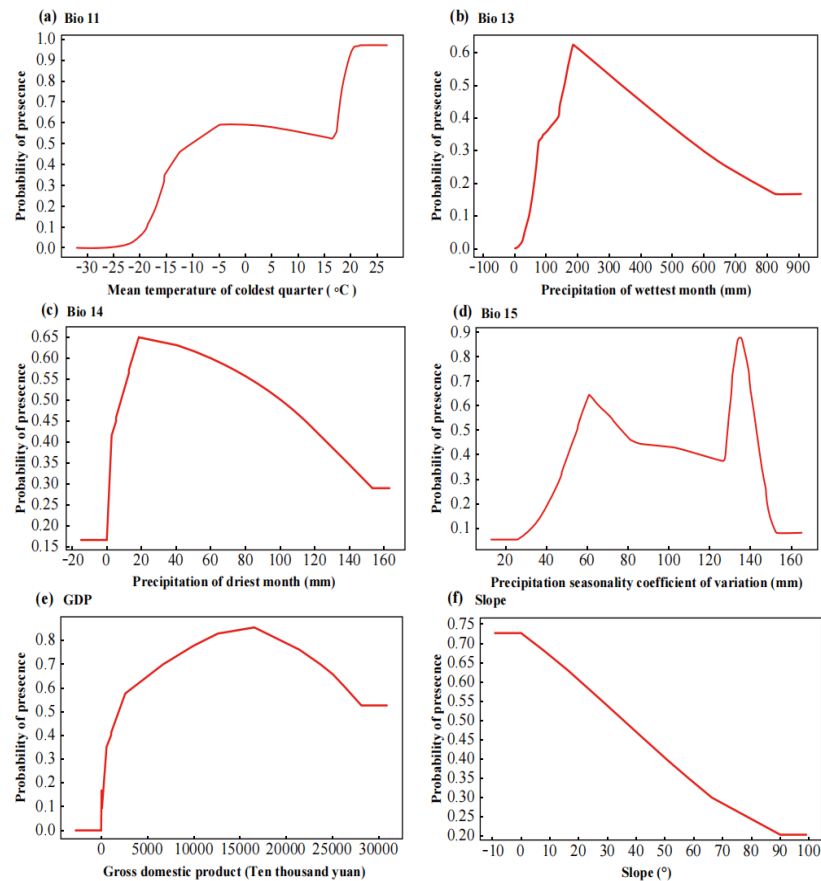


Figure 7. Response curves of asparagus-suitable area to the top six contributing environmental variables.

3.4. Spatial and Temporal Distribution Features of Suitable Areas for Asparagus in China Under Historical and Future Changes in Climate

The 14 key environmental factors were imported into the MaxEnt model to analyze the distribution of suitable habitats for Chinese asparagus under various historical and future climate scenarios (SSP585, SSP370, SSP245, and SSP126). In historical periods, the total suitable area was 345.6×10^5 km², which accounts for 36% of China's land area, primarily concentrated in Eastern China. In this area, the most suitable area was 40.3×10^5 km², mainly distributed in Hebei, Fujian, Shandong, Liaoning, Jiangsu, Henan, Shanxi, Shaanxi, Tianjin, Chongqing, and Sichuan. The medium-suitability area was 109.92×10^5 km², mostly located in the central regions of Shandong, Henan, and Shaanxi in China. The low-suitability zone covers an area of 192.51×10^5 km², primarily located in the southwest, southeast, and northeast regions of China (Figure 8j).

According to the MaxEnt model, the suitable areas for asparagus cultivation in China were predicted under various climate scenarios for the future periods of 2041–2060 (2050s), 2061–2080 (2070s), and 2081–2100 (2090s) (Figure 8a–l). It was projected that the asparagus-suitable area in the 2050s, 2070s, and 2090s under the SSP126 scenario was 373.52×10^5 , 379.62×10^5 , and 386.47×10^5 km², respectively. The distribution area of its suitable habitat was similar to that of the historical period, but the area had increased. Compared to the historical period, the suitable area increased by 27.92×10^5 km², 34.02×10^5 km², and 40.87×10^5 km², respectively. The additional suitable areas were mostly distributed in Hubei, Hunan, Zhejiang, and Jiangxi provinces. The suitable area for asparagus cultivation was 384.15×10^5 km², 400.11×10^5 km², and 386.70×10^5 km² in the 2050s, 2070s, and 2090s under the SSP245 scenario, respectively, i.e., an increase of 38.55×10^5 km², 54.51×10^5 km², and 41.60×10^5 km² compared to the historical period. The increased suitable growth areas were primarily distributed in Jiangxi, Hubei, and Hunan. Under the

SSP370 scenario, the suitable habitat area for asparagus was $373.83 \times 10^5 \text{ km}^2$, $402.48 \times 10^5 \text{ km}^2$, and $438.68 \times 10^5 \text{ km}^2$ in the future periods. It increased by $28.23 \times 10^5 \text{ km}^2$, $56.88 \times 10^5 \text{ km}^2$, and $93.08 \times 10^5 \text{ km}^2$ compared to the historical period, with the increased suitable areas being primarily distributed in Jiangxi, Hubei, Hunan, Zhejiang, Fujian, and Shanghai. The suitable habitat area for asparagus was $388.20 \times 10^5 \text{ km}^2$, $417.95 \times 10^5 \text{ km}^2$, and $437.52 \times 10^5 \text{ km}^2$ in the future period under the SSP585 scenario, respectively. This corresponds to an increase of $42.60 \times 10^5 \text{ km}^2$, $72.35 \times 10^5 \text{ km}^2$, and $91.92 \times 10^5 \text{ km}^2$ compared to the historical period. The increased suitable areas were primarily distributed in Hunan, Jilin, Liaoning, Shanghai, Jiangxi, Hubei, Zhejiang, and Fujian provinces (Table 3).

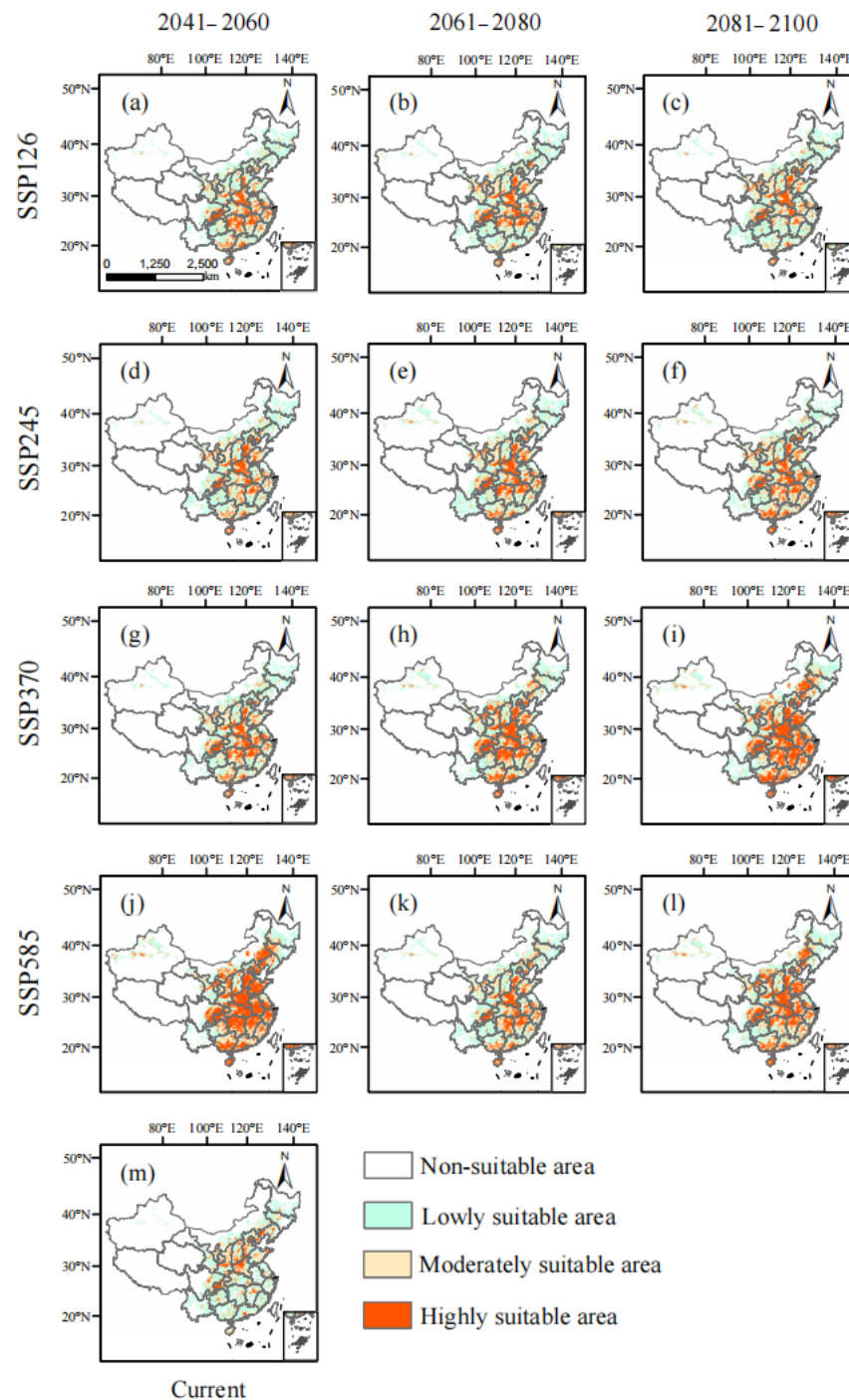


Figure 8. Suitable asparagus distribution areas in China under various historical (m) and future periods and climate scenarios (a–c, d–f, g–i, and j–l refer to the periods 2041–2060, 2061–2080, and 2081–2100 in the SSP126, SSP245, SSP370, and SSP5855 scenarios).

Table 3. The potential asparagus distribution areas in China under historical and CMIP6 future climate scenarios.

Climate Scenario	Period	Areas of Suitable Area (10 ⁵ km ²)			
		Unsuitable Area	Low-Suitability Area	Moderate-Suitability Area	High-Suitability Area
	1970–2000	614.40	192.51	111.92	41.17
SSP126	2041–2060	586.48	181.01	123.78	68.73
	2061–2080	580.38	186.85	126.75	66.02
	2081–2100	573.53	198.80	130.73	56.94
	2041–2060	575.85	189.62	133.18	61.35
SSP245	2061–2080	559.89	184.34	132.44	83.33
	2081–2100	573.30	168.78	131.44	86.48
	2041–2060	586.17	173.94	124.72	75.17
SSP370	2061–2080	557.52	154.25	134.29	113.94
	2081–2100	521.32	140.67	135.55	132.46
	2041–2060	571.80	179.33	132.50	76.37
SSP585	2061–2080	542.05	157.31	133.49	127.15
	2081–2100	522.48	125.69	127.31	184.52

The suitable regions for asparagus cultivation in China were primarily located in Jilin, Liaoning, eastern Inner Mongolia, southern Heilongjiang, southern Gansu, eastern Sichuan, and Hainan, as well as in the central and southeastern regions under SSP126, SSP245, SSP370, and SSP585 scenarios. There were also a few small, scattered patches distributed in Yunnan, Xinjiang, Tibet, and Qinghai (Figure 8). The trends in the total suitable area and highly suitable area from the historical period to the 2050s, the 2050s to the 2070s, and the 2070s to the 2090s show a consistent pattern, exhibiting a trend of increasing then decreasing then increasing again. Changes in unsuitable areas decreased from the present to the 2050s, increased from the 2050s to the 2070s, and then declined again from the 2070s to the 2090s (Table 4). The expansion range was mainly located in northeastern and southwestern China, as well as in certain regions in Xinjiang. In contrast, the contraction area was mainly located in southwestern Liaoning and northeastern Yunnan from the present day to the 2050s under various climate scenarios. From the 2050s to the 2070s, the contraction area decreased significantly compared to the historical to 2050s period, and the contraction area was mainly located in Liaoning and Jilin regions. During the period from the 2070s to the 2090s, there was a small increase in the contraction area, mainly concentrated in Yunnan and the eastern coastal regions (Figure 9).

Table 4. Relative variations in the area suitable for asparagus cultivation in China under various climate scenarios of CMIP6 for different periods in the future.

Climate Scenario		Area Variation (10 ⁵ km ²)		
		Current to 2041–2060	2041–2060 to 2061–2080	2061–2080 to 2081–2100
SSP126	Expansion area	84.43	17.29	24.47
	Non-habitable area	558.14	550.94	551.93
	Stability area	297.95	366.56	370.15
	Contraction area	19.48	25.21	13.45
SSP245	Expansion area	87.18	28.78	31.58
	Non-habitable area	545.52	541.76	515.65
	Stability area	324.19	384.88	397.25
	Contraction area	6.11	4.58	15.52
SSP370	Expansion area	88.66	67.21	41.21
	Non-habitable area	544.59	506.66	492.67
	Stability area	317.53	381.57	422.56

	Contraction area	9.22	4.56	3.56
	Expansion area	101.67	44.12	28.85
SSP585	Non-habitable area	530.85	512.39	491.35
	Stability area	321.36	396.32	432.04
	Contraction area	6.12	7.17	7.76

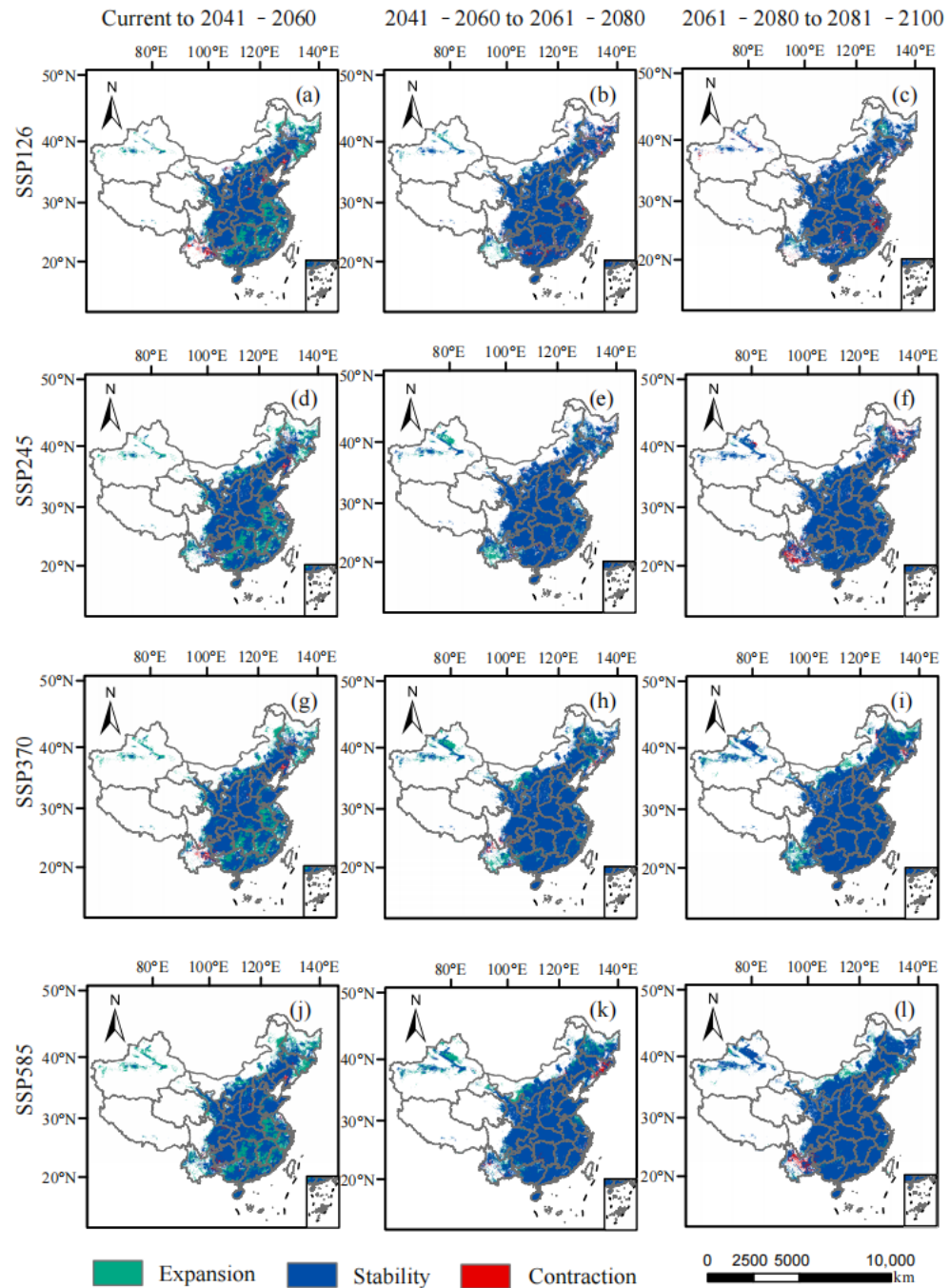


Figure 9. Variations in the suitable area pattern of asparagus in China under different future periods and climate scenarios (a–c, d–f, g–i, and j–l are the current to 2041–2060, 2041–2060 to 2061–2080, and 2061–2080 to 2081–2100 in the SSP126, SSP245, SSP370, and SSP585 scenarios).

3.5. Variations in the Centroid of Suitable Cultivation Areas for Asparagus in China Under Future Change in Climate

This study analyzed the centroid migration path of asparagus-suitable areas in both historical and various future climate scenarios. It was found that the center point of suitable areas for asparagus cultivation in China has a tendency to migrate northward in the future. As climate change intensifies in the future, the centroid migration of the asparagus-suitable area showed a trend of first becoming closer and then farther away, and the migration distance gradually increased (Figure 10).

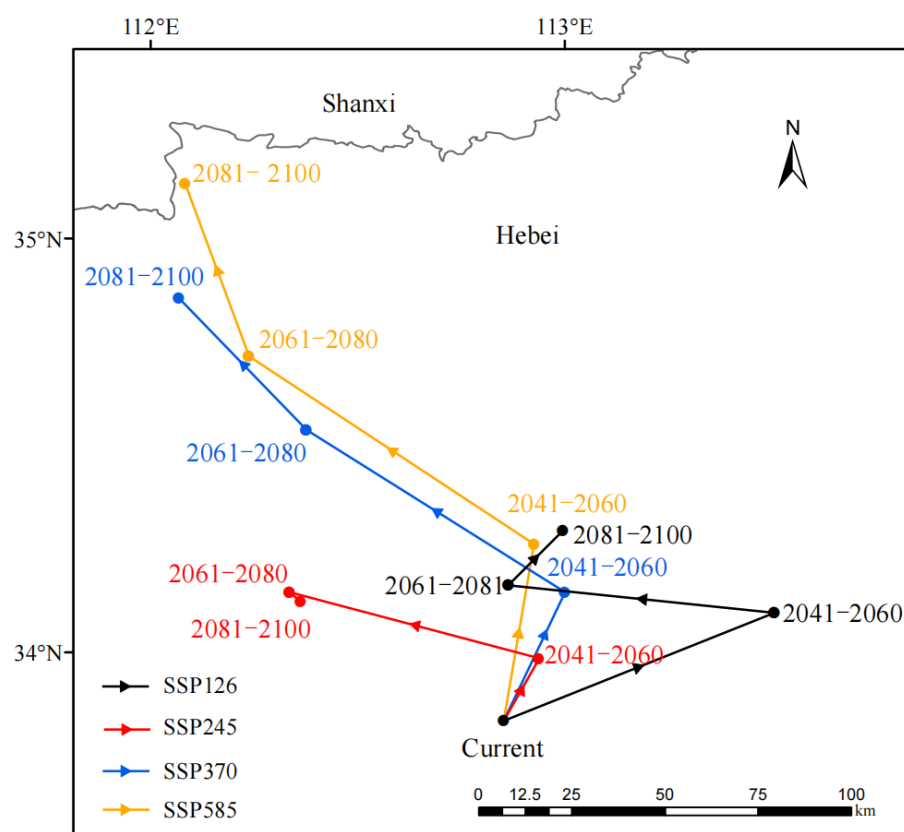


Figure 10. Future changes in center point migration of asparagus-suitable areas under various climate scenarios.

The center point of the suitable area for asparagus cultivation was located in the central-western Henan province (112.85° E, 33.84° N) (Figure 10). The centroid of asparagus suitable generally shifted northward under the SSP126 scenario. First, it shifted 67.82 km along the northeast to Xuchang city in Henan province (113.51° E, 34.11° N), followed by 60.04 km along the northwest to Pingdingshan city in Henan province (112.86° E, 34.16° N); then, it shifted 19.61 km along the northeast to Pingdingshan city in Henan province (112.99° E, 34.30° N). The centroid of asparagus generally shifted to the northwest under the SSP245 scenario. First, it moved 18.62 km along the northeast to Pingdingshan city in Henan province (112.94° E, 33.99° N), then moved 58.02 km along the northwest to Luoyang city in Henan province (112.34° E, 34.15° N), and then moved 2.89 km along the southwest to Luoyang city in Henan province (112.36° E, 34.13° N). Under the SSP370 scenario, the center point of the asparagus suitability zone also shifted, overall, to the northwest. First, it moved 37.12 km to Pingdingshan city in Henan province (113.00° E, 34.15° N) along the northeast direction, then move 71.51 km to Luoyang city in Henan province (112.38° E, 34.54° N) along the northwest direction, and then moved 45.46 km to

Luoyang city in Henan province (112.07° E, 34.86° N) along the northwest direction. The centroid generally shifted to the northwest in the SSP585 scenario. First, it moved 47.25 km in the northeast direction to Pingdingshan city in Henan province (112.93° E, 34.26° N), then moved 81.25 km in the northwest direction to Luoyang city in Henan province (112.24° E, 34.72° N), and finally moved 47.84 km in the northwest direction to Jiyuan city in Henan province (112.08° E, 35.13° N) (Table 5).

Table 5. The centroid distribution and migration distance of the asparagus-suitable area in China under various climate scenarios of CMIP6 in the future.

Climate Scenario	Period	Longitude (°)	Latitude (°)	Migration Period	Migration Distance (km)
SSP126	Current	112.85	33.84		
	2041–2060	113.51	34.11	Current to 2041–2060	67.82
	2061–2080	112.86	34.16	2041–2060 to 2061–2080	60.04
	2081–2100	112.99	34.30	2061–2080 to 2081–2100	19.61
SSP245	Current	112.85	33.84		
	2041–2060	112.94	33.99	Current to 2041–2060	18.62
	2061–2080	112.34	34.15	2041–2060 to 2061–2080	58.02
	2081–2100	112.36	34.13	2061–2080 to 2081–2100	2.89
SSP370	Current	112.85	33.84		
	2041–2060	113.00	34.15	Current to 2041–2060	37.12
	2061–2080	112.38	34.54	2041–2060 to 2061–2080	71.51
	2081–2100	112.07	34.86	2061–2080 to 2081–2100	45.46
SSP585	Current	112.85	33.84		
	2041–2060	112.93	34.26	Current to 2041–2060	47.25
	2061–2080	112.24	34.72	2041–2060 to 2061–2080	81.28
	2081–2100	112.08	35.13	2061–2080 to 2081–2100	47.84

4. Discussion

The MaxEnt model is a desirable model for predicting both actual and potential species distributions and is being employed more and more in invasion biology [45,46], conservation biology, and to determine the influences of global climate change on species distribution [47,48]. Although the widespread use of MaxEnt research often relies on default settings, i.e., without data processing and model parameterization, the model's accuracy is highly dependent on species sample information, environmental variable processing, and parameter settings [49]. In order to prevent overfitting from affecting model accuracy, this study processed asparagus distribution data using ENMTools software and environmental data using the Pearson correlation test. The Kuenm package for the R language was used to optimize the MaxEnt model. The optimized model accuracy was AUC = 0.931, which indicated that it could accurately predict the potential asparagus suitability zones in China.

Climate, terrain, soil, and human activities are the main environmental factors that determine species distribution [50–52]. This study indicated that precipitation (Bio13, Bio14, and Bio19), temperature (Bio3, Bio5, Bio8, and Bio11), slope, and GDP are the main environmental factors that affect the underlying geographic distribution of asparagus, cumulatively contributing 92.2%. GDP reflects the overall level of social and economic development, as well as shifts in market demand. With the growth of GDP, the increase in agricultural investment, the pull of consumer demand, and the progress and promotion of technology will encourage farmers to adjust the crop planting structure based on economic benefits and market prospects, thereby achieving higher output value and profit [53]. At the same time, factors including urbanization, environmental pollution, and ecological degradation will also put pressure on agricultural production and further affect

the crop planting distribution [54,55]. Asparagus has a strong adaptability to temperature, being both cold- and heat-resistant; when the soil temperature rises to 5 °C asparagus, will germinate; and it will grow normally at around 10 °C. The optimal temperature range for tender shoot formation is 15 °C to 17 °C. Low and high temperatures can inhibit photosynthesis and affect asparagus development [56]. The asparagus goes into summer dormancy when the temperature rises above 30 °C. The above- and underground parts enter dormancy for better overwintering when the winter temperatures in winter in the northern region are too low [57]. Although the well-developed root system of asparagus can withstand drought, it is susceptible to water-logging, and excessive precipitation can cause root rot [58,59]. Sloping cultivated land acts as a pivotal player in food production, ecosystem diversity, and economic development. Sloping affected soil depth, soil respiration, and nutrient utilization rates, with the asparagus survival threshold being greater than 0.5 when land slopes were less than 40°. Wang et al. [60] quantitatively analyzed the spatial distribution of 12 major crops on steep slopes (>12%) in Europe and found that steep-slope agriculture was vulnerable to drought. This study also found that gentler slopes were more suitable for the survival of asparagus. Human activities significantly affect global climate change, and the level of economic development levels plays a crucial role in agricultural productivity. Among anthropocentric factors, GDP has the greatest influence on the habitat's suitability for asparagus, contributing 71.6%. Identifying the main environmental factors that affect asparagus distribution, we can create rational zoning strategies to facilitate the introduction and cultivation of asparagus, as well as crop conservation.

This study found that future temperature change caused the centroid of the suitable areas for asparagus cultivation to shift northward, with a maximum migration distance of 67.82 km. The centroid shift suggests that the suitable areas for asparagus may change due to climate change, prompting farmers to adjust planting locations to adapt to the new climatic conditions. To ensure the sustainable development of asparagus, it will be essential to optimize water resource management and irrigation systems, as well as to adjust production seasons and land use practices. The suitable areas for asparagus had shifted to areas with less precipitation. This was highly consistent with the drought tolerance characteristics but not with the water logging tolerance characteristics of asparagus [61]. Additionally, moderate- and high-suitability areas for asparagus in China showed an increasing trend, while unsuitable and low-suitability areas exhibited a declining tendency under various future climatic scenarios. As the temperature increases, the suitable area for asparagus tends to increase, but there are limits to this expansion. Our findings suggested that the area unsuitable for asparagus in China is projected to increase from 2081 to 2100 under the SSP245 scenario, likely due to the rising temperature exceeding the suitable growth temperature range for asparagus.

The main distribution points in this study were derived from the specimen distribution information, which only indicated the existence of the species at specific locations. These data do not accurately reflect all of the distribution areas or potentially suitable habitats. However, due to the limitation in the available databases, the actual distribution area of asparagus may not be fully captured, and this study was mainly focused on China. The optimized MaxEnt model employed in this research can be employed in subsequent studies for predicting the global distribution of asparagus cultivation. Furthermore, this study relied solely on the MaxEnt model, and the results may be uncertain due to the influence of this model's structure. Future research could incorporate multiple species distribution models to analyze suitable areas for asparagus, thereby enhancing the reliability of their findings.

5. Conclusions

This research took into account the effects of soil, climate, topography, and human activity on asparagus cultivation distribution. Using the MaxEnt model and ArcGIS tools, the primary environmental parameters that influence the appropriate distribution for asparagus were determined. Additionally, this study forecasted and analyzed the spatio-temporal changes and variation in potential suitable areas for asparagus in China. The parameter-optimized MaxEnt model was found to be highly effective in predicting suitable areas for asparagus, with an AUC of 0.931. GDP, slope, Bio11, Bio13, Bio14, and Bio15 were the primary environmental factors that influenced the areas suitable for asparagus in China. Highly suitable areas for asparagus were located in Hebei, Fujian, Shandong, Liaoning, Jiangsu, Henan, Shanxi, Shaanxi, Tianjin, Chongqing, and Sichuan provinces in China. With the effect of future climate change, the suitable areas for asparagus are expected to expand. This expansion of suitable areas is focused on southwest China, northeast China, and certain parts of Xinjiang. Additionally, a few expansion zones were found in the Inner Mongolia, Qinghai, and Gansu provinces, while contraction zones were mainly found in northeastern Yunnan and southwest Liaoning province. Notably, the center points of the suitable areas for asparagus is projected to shift northward due to future climate change, but they were all located in Henan province. These findings can provide valuable guidance for planning asparagus cultivation, promoting the development of a high-quality and high-yield asparagus industry, and effectively addressing the challenges posed by climate change.

Author Contributions: C.J., writing—original draft, writing—review and editing, data curation, software; N.L., methodology, supervision, visualization, writing—review and editing; Q.Y., conceptualization, validation, funding acquisition; H.L. (Haixia Lin), data curation, visualization, validation; M.L., conceptualization, methodology, validation; H.L. (Haojie Li), investigation, methodology, resources; S.H., conceptualization, writing—review and editing, investigation; J.L., writing—review and editing, methodology, conceptualization. All authors have read and agreed to the published version of the manuscript.

Funding: This study was jointly funded by the National Natural Science Foundation of China (No. 52209055, 523799041); Yunnan Province College Students Innovation and Entrepreneurship Training Program Project Funding (S202310674099); International Joint Laboratory of Intelligent Agricultural Engineering Technology and Equipment in Yunnan Province (202403AP140007); Yunnan Field Scientific Observatory of Water-Soil-Crop Systems in Seasonal Dry Areas (202305AM070006); Applied Basic Research Key Project of Yunnan (No. 202201AS070034); Yunnan Science and Technology Talent and Platform Program (No. 202305AM070006); Yunnan Fundamental Research Projects (No. 202301AU070061); and the Yunnan Technology Innovation Center of Phosphorus Resource (No. 202305AK340002).

Institutional Review Board Statement: Not applicable.

Data Availability Statement: The raw data supporting the conclusions of this article will be made available by the authors on request.

Conflicts of Interest: The authors declare no conflicts of interest.

References

1. Dawid, C.; Hofmann, T. Identification of sensory-active phytochemicals in asparagus (*Asparagus officinalis* L.). *J. Agric. Food Chem.* **2012**, *60*, 11877–11888.
2. He, C.Y.; Hsiang, T.; Wolyn, D.J. Induction of systemic disease resistance and pathogen defence responses in *Asparagus officinalis* inoculated with nonpathogenic strains of *Fusarium oxysporum*. *Plant Pathol.* **2002**, *51*, 225–230.
3. Sharma, U.; Kumar, N.; Singh, B.; Munshi, R.K.; Bhalerao, S. Immunomodulatory active steroidal saponins from *Asparagus racemosus*. *Med. Chem. Res.* **2013**, *22*, 573–579.

4. Słupski, J.; Korus, A.; Lisiewska, Z.; Kmiecik, W. Content of amino acids and the quality of protein in as-eaten green asparagus (*Asparagus officinalis* L.) products. *Int. J. Food Sci. Technol.* **2010**, *45*, 733–739.
5. Chitrakar, B.; Zhang, M.; Adhikari, B. Asparagus (*Asparagus officinalis*): Processing effect on nutritional and phytochemical composition of spear and hard-stem byproducts. *Trends Food Sci. Technol.* **2019**, *93*, 1–11.
6. Liu, D.; Yan, F.; Liu, C.; Chen, A.; Wu, J.; Yu, M.; Lyu, X. Develo EST-SSR Markers for Identifying and Evaluating Asparagus Germplasm Resources Based on Transcriptome Sequences. *Horticulturae* **2024**, *10*, 121.
7. Guisan, A.; Thuiller, W. Predicting species distribution: offering more than simple habitat models. *Ecology Letters*, **2005**, *8*(9), 993–1009.
8. Forster, P.M.; Smith, C.J.; Walsh, T.; Lamb, W.F.; Lamboll, R.; Hauser, M.; Ribes, A.; Rosen, D.; Gillett, N.; Palmer, M.D.; et al. Indicators of Global Climate Change 2022: Annual update of large-scale indicators of the state of the climate system and human influence. *Earth Syst. Sci. Data* **2023**, *15*, 2295–2327.
9. Gregory, P.J.; Ingram, J.S.; Brklacich, M. Climate change and food security. *Philos. Trans. R. Soc. B Biol. Sci.* **2005**, *360*, 2139–2148.
10. Adhikari, D.; Barik, S.K.; Upadhaya, K. Habitat distribution modelling for reintroduction of *Ilex khasiana* Purk., a critically endangered tree species of northeastern India. *Ecol. Eng.* **2012**, *40*, 37–43.
11. Chardon, N.I.; Cornwell, W.K.; Flint, L.E.; Flint, A.L.; Ackerly, D.D. Topographic, latitudinal and climatic distribution of *Pinus coulteri*: Geographic range limits are not at the edge of the climate envelope. *Ecography* **2015**, *38*, 590–601.
12. Chen, I.C.; Hill, J.K.; Ohlemüller, R.; Roy, D.B.; Thomas, C.D. Rapid range shifts of species associated with high levels of climate warming. *Science* **2011**, *333*, 1024–1026.
13. Bowen, A.K.; Stevens, M.H. Temperature, topography, soil characteristics, and NDVI drive habitat preferences of a shade-tolerant invasive grass. *Ecol. Evol.* **2020**, *10*, 10785–10797.
14. Ling, X.; Zhang, Z.; Zhai, J.; Ye, S.; Huang, J. Advances in research on the effects of climate change on rice production in China. *Acta Crop. Sin.* **2019**, *45*, 323–334.
15. Unkovich, M.; McBeath, T.; Llewellyn, R.; Hall, J.; Gupta, V.V.; Macdonald, L.M. Challenges and opportunities for grain farming on sandy soils of semi-arid south and south-eastern Australia. *Soil Res.* **2020**, *58*, 323–334.
16. Atanasso, J.A.; Mensah, S.; Salako, K.V.; Tohoun, R.J.; Kakaï, R.G.; Assogbadjo, A.E. Factors affecting survival of seedling of *Azelia africana*, a threatened tropical timber species in West Africa. *Trop. Ecol.* **2021**, *62*, 443–452.
17. Ong, P.-W.; Lin, Y.-P.; Chen, H.-W.; Lo, C.-Y.; Burluyaeva, M.; Noble, T.; Nair, R.M.; Schafleitner, R.; Vishnyakova, M.; Bishop-Von-Wettberg, E.; et al. Environment as a limiting factor of the historical global spread of mungbean. *Elife* **2023**, *12*, e85725.
18. Higgins, S.I.; O'Hara, R.B.; Römermann, C. A niche for biology in species distribution models. *J. Biogeogr.* **2012**, *39*, 2091–2095.
19. Elith, J.; Leathwick, J.R. Species distribution models: Ecological explanation and prediction across space and time. *Annu. Rev. Ecol. Evol. Syst.* **2009**, *40*, 677–697.
20. Warren, D.L.; Seifert, S.N. Ecological niche modeling in Maxent: The importance of model complexity and the performance of model selection criteria. *Ecol. Appl.* **2011**, *21*, 335–342.
21. Hernandez, P.A.; Graham, C.H.; Master, L.L.; Albert, D.L. The effect of sample size and species characteristics on performance of different species distribution modeling methods. *Ecography* **2006**, *29*, 773–785.
22. Elith, J.H.; Graham, C.P.H.; Anderson, R.P.; Dudík, M.; Ferrier, S.; Guisan, A.; Hijmans, R.J.; Huettmann, F.; Leathwick, J.R.; Lehmann, A.; et al. Novel methods improve prediction of species distributions from occurrence data. *Ecography* **2006**, *29*, 129–151.
23. Fitzgibbon, A.; Pisut, D.; Fleisher, D. Evaluation of Maximum Entropy (Maxent) machine learning model to assess relationships between climate and corn suitability. *Land* **2022**, *11*, 1382.
24. Maguranyanga, C.; Murwira, A. Mapping maize, tobacco, and soybean fields in large-scale commercial farms of Zimbabwe based on multitemporal NDVI images in MAXENT. *Can. J. Remote Sens.* **2014**, *40*, 396–405.
25. Zhao, C.; Zhang, F.; Huang, J.; Zhang, Q.; Lu, Y.; Cao, W. Prediction of the Climatically Suitable Areas of Rice in China Based on Optimized MaxEnt Model. *Int. J. Plant Prod.* **2024**, *18*, 549–561.
26. Kogo, B.K.; Kumar, L.; Koech, R.; Kariyawasam, C.S. Modelling climate suitability for rainfed Maize cultivation in Kenya using a Maximum Entropy (MaxENT) approach. *Agronomy* **2019**, *9*, 727.
27. Yu, X.; Tao, X.; Liao, J.; Liu, S.; Xu, L.; Yuan, S.; Zhang, Z.; Wang, F.; Deng, N.; Huang, J.; et al. Predicting potential cultivation region and paddy area for ratoon rice production in China using Maxent model. *Field Crops Res.* **2022**, *275*, 108372.
28. Holder, A.M.; Markarian, A.; Doyle, J.M.; Olson, J.R. Predicting geographic distributions of fishes in remote stream networks using maximum entropy modeling and landscape characterizations. *Ecol. Model.* **2020**, *433*, 109231.

29. Halvorsen, R.; Mazzoni, S.; Bryn, A.; Bakkestuen, V. Opportunities for improved distribution modelling practice via a strict maximum likelihood interpretation of MaxEnt. *Ecography* **2015**, *38*, 172–183.
30. Montenegro, C.; Solitario, L.A.; Manglar, S.F.; Guinto, D.D. Niche modelling of endangered philippine birds using GARP and MAXENT. In Proceedings of the 2017 7th International Conference on Cloud Computing, Data Science & Engineering-Confluence, Noida, India, 12–13 January 2017; pp. 547–551.
31. Zhang, S.; Liu, X.; Li, R.; Wang, X.; Cheng, J.; Yang, Q.; Kong, H. AHP-GIS and MaxEnt for delineation of potential distribution of Arabica coffee plantation under future climate in Yunnan, China. *Ecol. Indic.* **2021**, *132*, 108339.
32. Warren, D.L.; Glor, R.E.; Turelli, M. ENMTools: A toolbox for comparative studies of environmental niche models. *Ecography* **2010**, *33*, 607–611.
33. Prasad, S.R.; Sharma, P. Species distribution modeling of asparagus (*Asparagus officinalis*) in India using MaxEnt model. *Environ. Monit. Assess.* **2020**, *192*, 518.
34. Yang, X.Q.; Kushwaha, S.P.S.; Saran, S.; Xu, J.; Roy, P.S. Maxent modeling for predicting the potential distribution of medicinal plant, *Justicia adhatoda* L. in Lesser Himalayan foothills. *Ecol. Eng.* **2013**, *51*, 83–87.
35. Phillips, S.J.; Dudík, M. Modeling of species distributions with Maxent: New extensions and a comprehensive evaluation. *Ecography* **2008**, *31*, 161–175.
36. Cobos, M.E.; Peterson, A.T.; Barve, N.; Osorio-Olvera, L. kuenm: An R package for detailed development of ecological niche models using Maxent. *PeerJ* **2019**, *7*, e6281.
37. Elith, J.; Leathwick, J.R.; Hastie, T. A working guide to boosted regression trees. *J. Anim. Ecol.* **2011**, *77*, 802–813.
38. Yu D, Deng L, Acero A. Using continuous features in the maximum entropy model. *Pattern Recognition Letters*, **2009**, *30*, 1295-1300.
39. Phillips, S.J.; Anderson, R.P.; Schapire, R.E. Maximum entropy modeling of species geographic distributions. *Ecol. Model.* **2006**, *190*, 231–259.
40. Anderson, R.P.; Lew, D.; Peterson, A.T. Evaluating predictive models of species' distributions: Criteria for selecting optimal models. *Ecol. Model.* **2003**, *162*, 211–232.
41. Symonds, M.R.; Moussalli, A. A brief guide to model selection, multimodel inference and model averaging in behavioural ecology using Akaike's information criterion. *Behav. Ecol. Sociobiol.* **2011**, *65*, 13–21.
42. Zhou, Y.; Lu, X.; Zhang, G. Potentially differential impacts on niche overlap between Chinese endangered *Zelkova schneideriana* and its associated tree species under climate change. *Front. Ecol. Evol.* **2023**, *11*, 1218149.
43. Jalaeian, M.; Golizadeh, A.; Sarafrazi, A.; Naimi, B. Inferring climatic controls of rice stem borers spatial distributions using maximum entropy modelling. *J. Appl. Entomol.* **2018**, *142*, 388–396.
44. Zhang, K.; Yao, L.; Meng, J.; Tao, J. Maxent modeling for predicting the potential geographical distribution of two peony species under climate change. *Sci. Total Environ.* **2018**, *634*, 1326–1334.
45. Morán Ordóñez, A.; Lahoz Monfort, J.J.; Elith, J.; Wintle, B.A. Evaluating 318 continental-scale species distribution models over a 60-year prediction horizon: What factors influence the reliability of predictions? *Glob. Ecol. Biogeogr.* **2017**, *26*, 371–384.
46. Wan, J.Z.; Wang, C.J.; Yu, F.H. Effects of occurrence record number, environmental variable number, and spatial scales on MaxEnt distribution modelling for invasive plants. *Biologia* **2019**, *74*, 757–766.
47. Searcy, C.A.; Shaffer, H.B. Do ecological niche models accurately identify climatic determinants of species ranges? *Am. Nat.* **2016**, *187*, 423–435.
48. Sutton, G.F.; Martin, G.D. Testing MaxEnt model performance in a novel geographic region using an intentionally introduced insect. *Ecol. Model.* **2022**, *473*, 110139.
49. Song, R.; Ma, Y.; Hu, Z.; Li, Y.; Li, M.; Wu, L.; Li, C.; Dao, E.; Fan, X.; Hao, Y.; et al. MaxEnt modeling of *Dermacentor marginatus* (Acari: Ixodidae) distribution in Xinjiang, China. *J. Med. Entomol.* **2020**, *57*, 1659–1667.
50. Cardoza-Martínez, G.F.; Becerra-López, J.L.; Esparza-Estrada, C.E.; Estrada-Rodríguez, J.L.; Czaja, A.; Ehsan, M.; Baltierra-Trejo, E.; Romero-Méndez, U. Shifts in Climatic Niche Occupation in *Astrophytum Coahuilense* (H. Möller) Kayser and Its Potential Distribution in Mexico. *Sustainability* **2019**, *11*, 1138.
51. Davis, M.B.; Shaw, R.G. Range shifts and adaptive responses to Quaternary climate change. *Science* **2001**, *292*, 673–679.
52. Pajunen, V.; Luoto, M.; Soininen, J. Climate is an important driver for stream diatom distributions. *Glob. Ecol. Biogeogr.* **2016**, *25*, 198–206.
53. Smith, J.; Johnson, M.; Lee, H. Economic development and agricultural restructuring: A global perspective. *Agric. Econ. Rev.* **2015**, *42*, 67–82.
54. Zhang, Y.; Li, X. Impact of urbanization on agricultural production: A case study in China. *J. Rural. Dev.* **2018**, *29*, 145–160.

55. Zhou, T.; Liu, S.; Wang, F. Environmental degradation and its effect on crop distribution in China. *Environ. Sci. Technol.* **2020**, *54*, 5724–5733.
56. Radosavljevic, A.; Anderson, R.P. Making better Maxent models of species distributions: Complexity, overfitting and evaluation. *J. Biogeogr.* **2014**, *41*, 629–643.
57. Short, W.; Wolyn, D.J. The role of drought stress on the acquisition of freezing tolerance in asparagus under controlled conditions. *Can. J. Plant Sci.* **2022**, *102*, 864–874.
58. Drost, D.; Wilcox-Lee, D. Tillage alters root distribution in a mature asparagus planting. *Sci. Hortic.* **2000**, *83*, 187–204.
59. Namaki, A.; Ghahremani, Z.; Aelaei, M.; Barzegar, T.; Ranjbar, M.E. The first report of drought tolerance assessment of Iranian asparagus. *Gesunde Pflanz.* **2022**, *74*, 141–149.
60. Wang, W.; Straffelini, E.; Tarolli, P. 44% of steep slope cropland in Europe vulnerable to drought. *Geogr. Sustain.* **2024**, *5*, 89–95.
61. Mantovani, D.; Rosati, A.; Perrone, D. Photosynthetic characterization and response to drought and temperature in wild asparagus (*Asparagus acutifolius* L.). *HortScience* **2019**, *54*, 1039–1043.

Disclaimer/Publisher’s Note: The statements, opinions and data contained in all publications are solely those of the individual author(s) and contributor(s) and not of MDPI and/or the editor(s). MDPI and/or the editor(s) disclaim responsibility for any injury to people or property resulting from any ideas, methods, instructions or products referred to in the content.